  Bull. Chem. Soc. Jpn., 59, 515—523 (1986)

Transformation between Lamellar and Nonlamellar Aggregates Formed with Synthetic Peptide Lipids†

Yukito MURAKAMI,* Jun-ichi KIKUCHI, Toshihiko TAKAKI, and Katsuya UCHIMURA
Department of Organic Synthesis, Faculty of Engineering, Kyushu University, Hakozaki, Higashi-ku, Fukuoka 812
(Received September 30, 1985)

The morphological behavior of various combinations of the following synthetic lipids was investigated in the aqueous dispersion state by means of electron microscopy, differential scanning calorimetry, and fluorescence polarization spectroscopy as well as by turbidity and X-ray diffraction measurements: $N^+C_5Ala2C_n$ and $N^+(H)C_5Ala2C_n$ as cationic, $(SO_3^-)C_5Ala2C_n$ as anionic, and QC_5Ala2C_n as nonionic (n=14, 16). Aqueous dispersions of various combinations of cationic and anionic lipids at the equimolar ratio afforded nonlamellar aggregates, having highly ordered and three-dimensional network structure with repeating distances in the 70—130 Å range, above their phase transition temperatures (T_m). However, any slight loss of the fractional balance retained at the equimolar ratio led to the formation of bilayer aggregates. Under such conditions that allow the formation of nonlamellar aggregates, the high microscopic homogeneity of cationic and anionic lipid molecules was attained, originating from the intramembrane electrostatic interaction between cationic and anionic head moieties to form highly developed ion-pair clusters on the aggregate surface. Meanwhile, the nonlamellar phase appeared above T_m was spontaneously transformed into the normal bilayer phase below T_m as confirmed by electron microscopy and turbidity measurements. The nonlamellar phase was also characterized by the low-angle X-ray diffraction method and was consistent with the highly developed domain with the face-centered cubic lattice.

The polymorphic phase behavior has been found to arise by changing compositions and properties of membrane-forming lipids in the aqueous dispersion state.[1] In contrast with extensive studies on the bilayer phase, characterization of the nonbilayer ones, such as inverted hexagonal (H_{II}), lipidic particle (LIP), and inverted cubic (C_{II}) phases, has been limited to systems composed of naturally occurring lipids up to the present time.[2] In connection with dynamic functions of biomembranes, the correlations between lipid compositions and morphological transitions between bilayer and nonbilayer phases pose major unsolved subjects.[2,3] In this regard, simple model systems composed of synthetic lipids may make useful contributions toward general understanding of biological phenomena. Although various bilayer-forming lipids have been prepared,[4] synthetic lipids capable of forming nonbilayer aggregates under diluted conditions in aqueous media have been scarcely treated. Recently, we have found that a series of ionic peptide lipids involving an amino acid residue interposed between a polar head group and an aliphatic double-chain segment form bilayer membranes (vesicles and/or lamellae) in the aqueous dispersion state.[5] On the other hand, nonionic lipids having the quinoyl group as a polar head have been confirmed to form nonlamellar network aggregates when they were dispersed in aqueous media.[6] As described in our preliminary communication,[7] the similar morphology was also observed for equimolar mixtures of cationic and anionic peptide lipids.

In order to understand the molecular basis for formation of nonlamellar aggregates, the morphological behavior of various combinations of the following synthetic lipids was investigated in the aqueous dispersion state: $N^+C_5Ala2C_n$ and $N^+(H)C_5Ala2C_n$ as cationic, $(SO_3^-)C_5Ala2C_n$ as anionic, and QC_5Ala2C_n as nonionic (n=14, 16).

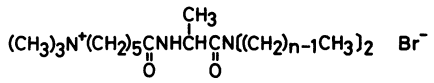

$N^+C_5Ala2C_n$ (n = 14,16)

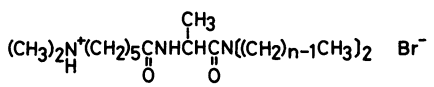

$N^+(H)C_5Ala2C_n$ (n = 14,16)

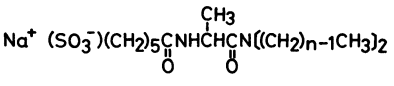

$(SO_3^-)C_5Ala2C_n$ (n = 14,16)

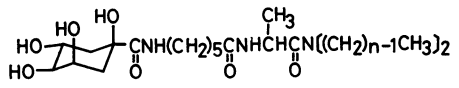

QC_5Ala2C_n (n = 14,16)

Experimental

Materials. 1,6-Diphenyl-1,3,5-hexatriene (DPH) was obtained from Nakarai Chemicals as a guaranteed reagent and used without further purification. The preparation of the following lipids has been reported previously: *N,N*-ditetradecyl-N^α-[6-(trimethylammonio)hexanoyl]-L-alaninamide bromide ($N^+C_5Ala2C_{14}$),[5c] *N,N*-dihexadecyl-N^α-[6-(trimethylammonio)hexanoyl]-L-alaninamide bromide ($N^+C_5Ala2C_{16}$),[5c] sodium *N,N*-ditetradecyl-N^α-(6-sulfohexanoyl)-L-alaninamide [$(SO_3^-)C_5Ala2C_{14}$],[6b] sodium *N,N*-dihex-

†Contribution No. 778 from this Department.

adecyl-N^{α}-(6-sulfohexanoyl)-L-alaninamide [$(SO_3^-)C_5Ala2C_{16}$],[6b] *N,N*-ditetradecyl-N^{α}-[6-(quinoylamino)hexanoyl]-L-alaninamide (QC_5Ala2C_{14}),[6a)#] and *N,N*-dihexadecyl-N^{α}-[6-(quinoylamino)hexanoyl]-L-alaninamide (QC_5Ala2C_{16}).[6b)#]

***N,N*-Ditetradecyl-N^{α}-[6-(dimethylamino)hexanoyl]-L-alaninamide (NC_5Ala2C_{14}).** This material was prepared in a manner similar to that reported for the synthesis of *N,N*-didodecyl-N^{α}-[6-(dimethylamino)hexanoyl]-L-alaninamide,[5b] and isolated as the hydrobromide salt [$N^+(H)C_5Ala2C_{14}$]: a white glassy solid, final mp 123 °C; $[\alpha]_D^{25}$ −15.0° (*c* 1.01, ethanol); IR (KBr) 2920 and 2850 (CH), and 1640 cm^{-1} (C=O); ^{1}H-NMR ($CDCl_3$, TMS) δ=0.88 [6H, br t, $(CH_2)_{13}C\underline{H}_3$], 1.0—2.0 [57H, m, $CH_2(C\underline{H}_2)_{12}CH_3$, $CH(C\underline{H}_3)$, and $CH_2(C\underline{H}_2)_3CH_2CO$], 2.28 [2H, br t, CH_2CO], 2.81 [6H, s, $(C\underline{H}_3)_2HN^+$], 2.9—3.8 [6H, m, N^+CH_2 and $NC\underline{H}_2(CH_2)_{12}CH_3$], 4.80 [1H, m, $C\underline{H}(CH_3)$], and 6.83 [1H, d, CONH].

Found: C, 66.40; H, 11.42; N, 5.75. Calcd for $C_{39}H_{79}N_3O_2\cdot$HBr: C, 66.63; H, 11.47; N, 5.98.

***N,N*-Dihexadecyl-N^{α}-[6-(dimethylamino)hexanoyl]-L-alaninamide (NC_5Ala2C_{16}).** This material was prepared in a manner as described above and isolated as the hydrobromide salt [$N^+(H)C_5Ala2C_{16}$]: a white glassy solid, final mp 126 °C; $[\alpha]_D^{25}$ −20.8° (*c* 1.01, ethanol); IR (KBr) 2920 and 2850 (CH), and 1640 cm^{-1} (C=O); ^{1}H-NMR ($CDCl_3$, TMS) δ=0.87 [6H, br t, $(CH_2)_{15}C\underline{H}_3$], 1.0—2.0 [65H, m, $CH_2(C\underline{H}_2)_{14}CH_3$, $CH(C\underline{H}_3)$, and $CH_2(C\underline{H}_2)_3CH_2CO$], 2.25 [2H, br t, CH_2CO], 2.80 [6H, s, $(C\underline{H}_3)_2HN^+$], 2.9—3.7 [6H, m, N^+CH_2 and $NC\underline{H}_2(CH_2)_{14}CH_3$], 4.79 [1H, m, $C\underline{H}(CH_3)$], and 6.77 [1H, d, CONH].

Found: C, 68.16; H, 11.80; N, 5.55. Calcd for $C_{43}H_{87}N_3O_2\cdot$HBr: C, 68.03; H, 11.68; N, 5.54.

Preparation of Molecular Aggregates. As for mixed lipid systems, chloroform solutions of two different lipids were mixed at appropriate molar ratios and evaporated to dryness to give thin films. Each film placed in 2 mL of deionized and distilled water was subjected to vortex mixing with glass beads at room temperature (ca. 20 °C) for 1—10 min to afford an aqueous dispersion sample. Whenever necessary, the dispersion sample was subsequently sonicated with a probe-type (W-220F, Heat Systems-Ultrasonics) or a bath-type sonicator (Bransonic 12, Yamato Scientific Co.) and allowed to stand for 20 min at room temperature.

Analyses and Measurements. Elemental analyses were performed at the Microanalysis Center of Kyushu University. Melting points were measured with a Yanagimoto MP-S1 apparatus (hot-plate type). IR spectra were recorded on a JASCO IR-810 spectrophotometer. ^{1}H-NMR spectra were taken on a Hitachi R-24B or a Hitachi Perkin-Elmer R-20 spectrometer. Turbidity measurements were run at 400 nm on a Hitachi 340 or a Union Giken SM-401 high sensitivity spectrophotometer with a cell of 1.0-mm path length. A Daini Seikosha SSC-560U calorimeter was used for differential scanning calorimetry (DSC). The phase transition temperature (T_m, temperature at a peak maximum of DSC thermogram) and the enthalpy change for phase transition (ΔH) were determined in the same manner as reported previously.[6b] Electron micrographs were taken on a JEOL JEM-200B electron microscope installed at the Research Laboratory for High Voltage Electron Microscopy of Kyushu University. The negatively stained samples for the measurements were prepared in a manner as described previously.[6b]

The fluorescence polarization measurements were carried out on a Union Giken FS-501A fluorescence polarization spectrophotometer equipped with a Sord microcomputer M200 Mark II; the emission at 450 nm originated from DPH was monitored upon excitation at 366 nm with a slit width of 3.5 nm for both excitation and emission sides. The steady-state fluorescence anisotropy (r_s) was calculated by Eq. 1, where I is the fluorescence intensity, and the subscripts v and h refer to the orientations, vertical and horizontal, respectively, for the excitation and analyzer polarizers in this sequence. C_f is the grating correction factor, given by I_{hv}/I_{hh}.

$$r_s=(I_{vv}-C_fI_{vh})/(I_{vv}+2C_fI_{vh}) \quad (1)$$

The nickel-filtered Cu $K\alpha$ radiation (λ=1.5418 Å) from a Rigaku Rotaflex RU-200 X-ray generator was used for X-ray diffraction measurements. Each sample was sealed up in a specimen holder equipped with mica windows, and a low-angle diffraction pattern was recorded on a Fuji X-ray film 150; a sample—film distance being set at 200 mm.

Results

Electron Microscopy. We have previously reported aggregate morphology of the following individual lipids in aqueous media: $N^+C_5Ala2C_n$,[5c] $(SO_3^-)C_5Ala2C_n$,[6b] and QC_5Ala2C_n.[6] Additional lipids having the amino group, NC_5Ala2C_n (n=14, 16), were prepared in this work and found to behave as cationic lipids under acidic conditions (below pH 6) that allow the amino head moiety to be protonated, $N^+(H)C_5Ala2C_n$.[8] The cationic $N^+(H)C_5Ala2C_n$ was found to constitute multilayered aggregates, bent lamellae and vesicles (Fig. 1A), in the aqueous dispersion state and single-walled vesicles in the diameter range 200—1000 Å (Fig. 1B) after treated with a probe-type sonicator for 2 min at 30 W.

When equimolar amounts of a cationic lipid, $N^+(H)C_5Ala2C_{16}$, and an anionic one, $(SO_3^-)C_5Ala2C_{14}$, were dispersed in water at pH 4.0 and 20 °C, the formation of nonlamellar aggregates was detected by electron microscopy with the negative staining technique; highly ordered network structure with a repeating distance of 100 Å (Fig. 2A). Similar aggregates with repeating distances in the 70—130 Å range were observed in aqueous dispersions of the following combinations of cationic and anionic lipids at the equimolar ratio above their phase transition temperatures; $N^+C_5Ala2C_{14}$-$(SO_3^-)C_5Ala2C_{14}$,[7] $N^+C_5Ala2C_{16}$-$(SO_3^-)C_5Ala2C_{16}$, $N^+(H)C_5Ala2C_{14}$-$(SO_3^-)C_5Ala2C_{14}$, $N^+(H)C_5Ala2C_{14}$-$(SO_3^-)C_5Ala2C_{16}$ (Fig. 2B), and $N^+(H)C_5Ala2C_{16}$-$(SO_3^-)C_5Ala2C_{16}$. Such characteristic morphological behavior was also confirmed by the freeze-fracture electron microscopy as typically shown for the $N^+C_5Ala2C_{14}$-$(SO_3^-)C_5Ala2C_{14}$ system; close

Quinoyl is the conventional name for 1,3,4,5-tetrahydroxy-[1*R*-(1α, 3α, 4α, 5β)]cyclohexylcarbonyl.

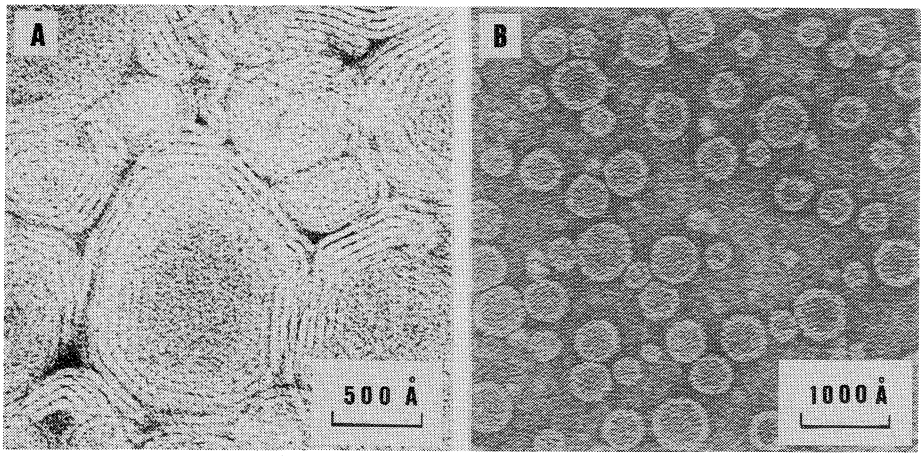

Fig. 1. Electron micrographs negatively stained with uranyl acetate: A, 5 mmol dm^{-3} aqueous dispersion of $N^+(H)C_5Ala2C_{14}$; B, 5 mmol dm^{-3} aqueous solution of $N^+(H)C_5Ala2C_{16}$ sonicated for 2 min with a probe-type sonicator at 30 W.

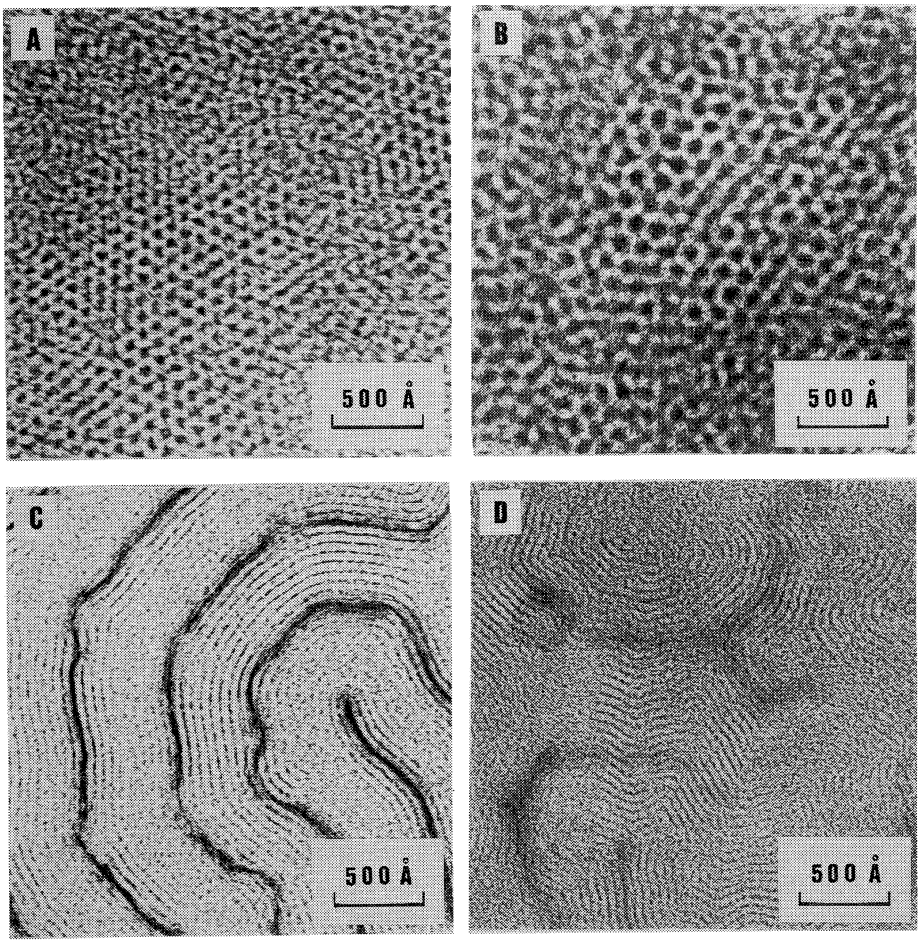

Fig. 2. Electron micrographs for equimolar mixtures (2.5 mmol dm^{-3} each) of two peptide lipids with the following combinations in the dispersion state, as negatively stained with uranyl acetate: A, $N^+(H)C_5Ala2C_{16}$ and $(SO_3^-)C_5Ala2C_{14}$; B, $N^+(H)C_5Ala2C_{14}$ and $(SO_3^-)C_5Ala2C_{16}$; C, $N^+(H)C_5Ala2C_{14}$ and $N^+C_5Ala2C_{16}$; D, QC_5Ala2C_{14} and $(SO_3^-)C_5Ala2C_{16}$.

packing of globular aggregates.[7] On the other hand, other mixed lipid systems, containing two kinds of peptide lipids at the equimolar ratio, formed normal bilayer aggregates in the aqueous dispersion state; e.g., $N^+C_5Ala2C_n$–$N^+(H)C_5Ala2C_n$ (Fig. 2C), N^+-C_5Ala2C_n–QC_5Ala2C_n, $N^+(H)C_5Ala2C_n$–QC_5Ala2C_n,

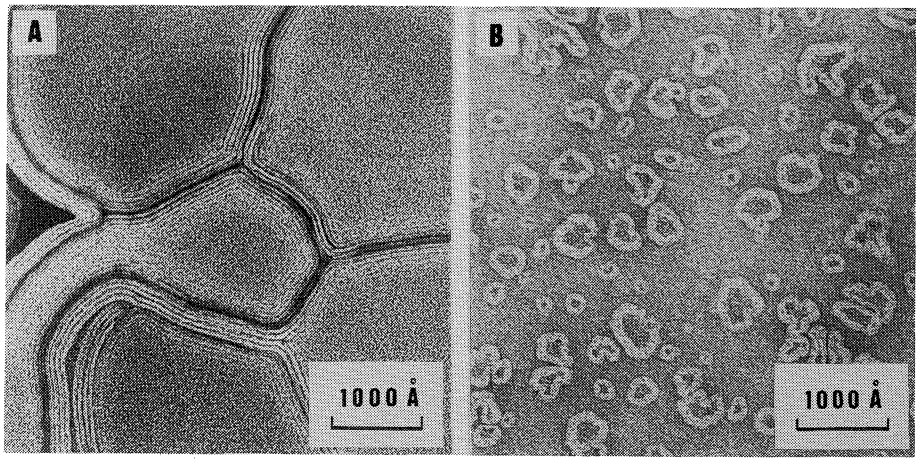

Fig. 3. Electron micrographs for a mixture of $N^+(H)C_5Ala2C_{14}$ (3.75 mmol dm^{-3}) and $(SO_3^-)C_5Ala2C_{14}$ (1.25 mmol dm^{-3}), as negatively stained with uranyl acetate: A, aqueous dispersion; B, aqueous solution sonicated for 60 min with a bath-type sonicator at 30 W.

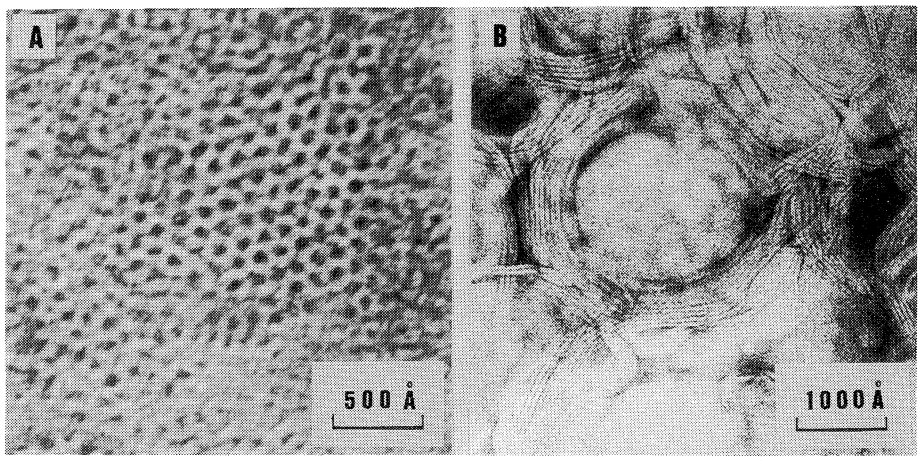

Fig. 4. Electron micrographs for an equimolar mixture (2.5 mmol dm^{-3} each) of $N^+C_5Ala2C_{16}$ and $(SO_3^-)C_5Ala2C_{16}$ in the dispersion state, as negatively stained with uranyl acetate: A, prepared at 50 °C; B, prepared at 5 °C.

and QC_5Ala2C_n-$(SO_3^-)C_5Ala2C_n$ (Fig. 2D). As for the systems composed of cationic and anionic lipids, any slight loss of the fractional balance retained at the equimolar ratio leads to the formation of bilayer aggregates. For example, bent lamellae were observed in an aqueous dispersion of $N^+(H)C_5Ala2C_{14}$ and $(SO_3^-)C_5Ala2C_{14}$ at the 3:1 molar ratio (Fig. 3A) and converted into single-walled vesicles in the diameter range 200—600 Å upon sonication with a bath-type sonicator for 60 min at 30 W (Fig. 3B). It needs to be noted that the aggregate morphology is subjected to change by the temperature range adopted for investigation, even if both cationic and anionic lipids were mixed exactly at the equimolar ratio, and the nonlamellar network aggregates were observed above the gel-liquid crystalline phase transition temperature. For example, the $N^+C_5Ala2C_{16}$-(SO_3^-)-C_5Ala2C_{16} system, T_m at 27.0 °C (vide infra), formed nonbilayer and bilayer aggregates at 50 and 5 °C, respectively, in the dispersion state as shown in Fig. 4.

Differential Scanning Calorimetry (DSC). The phase transition parameters (maximum temperature, T_m; enthalpy change, ΔH) for the bilayer aggregates formed with individual ionic lipids in the aqueous dispersion state are linearly correlated with the size of double-chain segment,[5c] and the nature of the head group segments has little effect on the parameters.[6b] The T_m and ΔH values for the cationic bilayer aggregates composed of $N^+(H)C_5Ala2C_n$ at pH 6 are 1.3 °C and 17.6 kJ mol^{-1} for n=14 and 24.8 °C and 27.6 kJ mol^{-1} for n=16, respectively. These values are comparable to those observed for other ionic bilayer aggregates having the same double-chain segments.[6b]

The phase transition parameters for the mixed lipid systems are listed in Table 1. It is clear that the T_m value is primarily dependent on the size and combination of the double-chain segments. The aggregate composed of two different lipids having the same double-chain segment shows a T_m value comparable to those for the aggregates of individual lipids, whereas the aggregate

Table 1. Phase Transition Parameters for Homogeneous Lipid Mixtures in Aqueous Dispersion

Mixed lipid system[a]	T_m/°C (ΔH/kJ mol^{-1})[b]			
	$m=n=14$	$m=14$, $n=16$	$m=16$, $n=14$	$m=n=16$
$N^+(H)C_5Ala2C_m/N^+C_5Ala2C_n$	2.0 (18.4)		16.1	25.3 (31.4)
$N^+C_5Ala2C_m/QC_5Ala2C_n$		13.9	14.2 (26.8)	
$QC_5Ala2C_m/(SO_3^-)C_5Ala2C_n$	2.3 (12.6)	15.3 (17.6)	14.3 (20.1)	
$N^+C_5Ala2C_m/(SO_3^-)C_5Ala2C_n$	4.9 (13.0)		15.5 (25.5)	27.0 (25.9)
$N^+(H)C_5Ala2C_m/(SO_3^-)C_5Ala2C_n$	4.3 (13.4)	14.2 (18.0)		27.0 (27.2)

a) Concentration of each lipid, 2.5 mmol dm^{-3}. b) ΔH values are given in parentheses. Each system without ΔH showed a broad peak which makes it difficult to evaluate the accurate value.

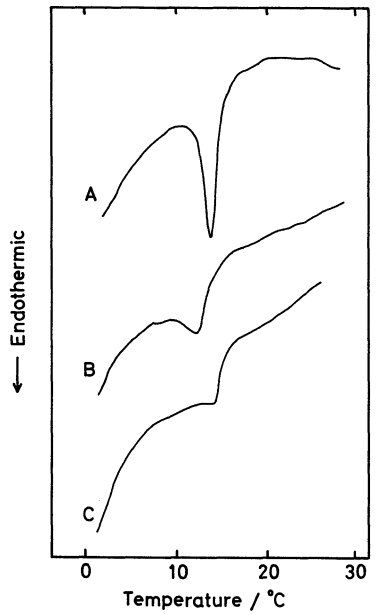

Fig. 5. DSC thermograms for equimolar mixtures (2.5 mmol dm^{-3} each) of two peptide lipids with the following combinations in the dispersion state: A, $N^+C_5Ala2C_{16}$ and $(SO_3^-)C_5Ala2C_{14}$; B, $N^+(H)$-C_5Ala2C_{16} and $N^+C_5Ala2C_{14}$; C, $N^+C_5Ala2C_{14}$ and QC_5Ala2C_{16}.

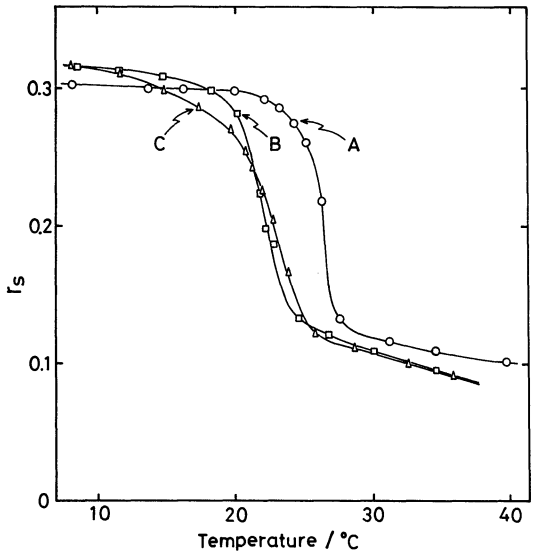

Fig. 6. Correlations of steady-state fluorescence anisotropy r_s with temperature for DPH (1.0×10^{-7} mol dm^{-3}) embedded in the following aggregates at pH 6.0: A, an equimolar mixture (2.5 mmol dm^{-3} each) of $N^+(H)C_5Ala2C_{16}$ and $(SO_3^-)C_5Ala2C_{16}$; B, 5 mmol dm^{-3} $N^+(H)C_5Ala2C_{16}$; C, 5 mmol dm^{-3} $(SO_3^-)C_5Ala2C_{16}$.

formed with an equimolar mixture of two kinds of lipids having different double-chain segments provides a phase transition peak in an intermediate region between intrinsic peaks of the individual aggregates. The ΔH values for the mixed lipid systems, which involve single species of the double-chain segments, are nearly identical with those for the corresponding bilayer aggregates of individual lipids.

The electrostatic interaction mode effective in the polar aggregate domain is reflected on the DSC thermographic pattern when the aggregate is composed of two kinds of peptide lipids having different double-chain segments. As shown in Fig. 5, the 1:1 cationic-anionic lipid system exhibits a sharp phase transition peak as compared with those for other mixed lipid systems. This undoubtedly indicates that highly homogeneous mixing of the cationic and anionic lipids is attained and consequently the surface charge is effectively neutralized without phase separation through formation of tight ion-pairs.

Fluorescence Polarization Spectroscopy. The steady-state fluorescence anisotropy (r_s) of 1,6-diphenyl-1,3,5-hexatriene (DPH) embedded in various aggregates is shown in Fig. 6 for selected cases as a function of temperature. The T_m value for an equimolar mixture of $N^+(H)C_5Ala2C_{16}$ and $(SO_3^-)C_5Ala2C_{16}$ was obtained from the inflection range (27 °C) and is in good agreement with that evaluated by DSC. The extent of variation of r_s for the mixed lipid system is comparable to those for the individual lipid systems over a whole temperature range studied.

Turbidity Measurements. The nonlamellar aggregates formed with both cationic and anionic lipids together provide largely developed domains (2000—20000 Å)[7] as reflected on the extent of turbidity which is appreciably larger than those observed for individual bilayer membranes in the dispersion state. Correlations of turbidity with temperature for aqueous dispersions of some mixed lipid systems are shown in Fig. 7. The bilayer aggregates, composed of $N^+C_5Ala2C_{16}$-$N^+(H)C_5Ala2C_{16}$ and (SO_3^-)-C_5Ala2C_{16}-QC_5Ala2C_{16}, do not undergo any turbidi-

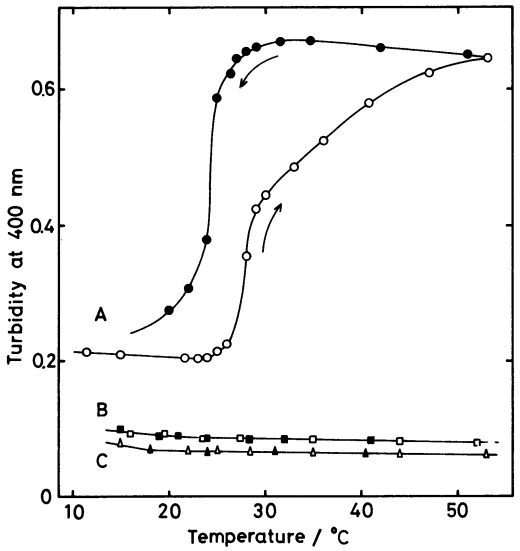

Fig. 7. Correlations of turbidity with temperature for equimolar mixtures (2.5 mmol dm^{-3} each) of two peptide lipids with the following combinations in the dispersion state: A, $N^+(H)C_5Ala2C_{16}$ and $(SO_3^-)C_5Ala2C_{16}$; B, $N^+(H)C_5Ala2C_{16}$ and $N^+C_5Ala2C_{16}$; C, QC_5Ala2C_{16} and $(SO_3^-)C_5Ala2C_{16}$. The values observed in heating and cooling processes are indicated with open and closed circles, respectively, and the measurements were carried out after incubation for 30 min at respective temperatures.

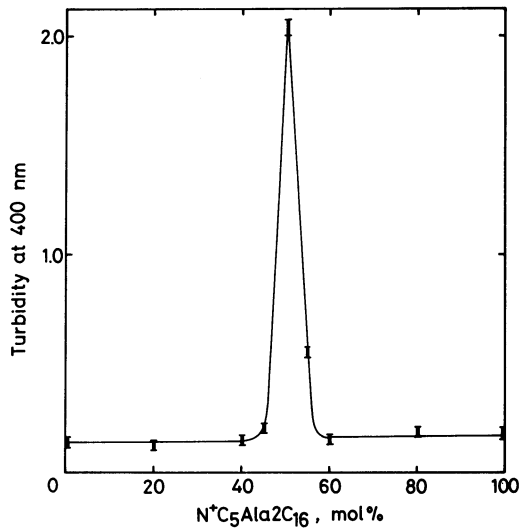

Fig. 8. Correlation of lipid composition with turbidity in the dispersion state for the homogeneously mixed system of $N^+C_5Ala2C_{16}$ and $(SO_3^-)C_5Ala2C_{16}$ at 30 °C; total lipid concentration, 5.0 mmol dm^{-3}.

ty change over the whole temperature range regardless of the phase transition. On the other hand, turbidity of the $N^+(H)C_5Ala2C_{16}$–$(SO_3^-)C_5Ala2C_{16}$ system is subjected to change in a sigmoidal manner with a hysteresis effect as shown in Fig. 7. The inflection range for turbidity change apparently corresponds to the phase transition temperature, and the turbidity observed below T_m is comparable to that for the bilayer aggregates. A similar correlation of turbidity with temperature was observed for the aqueous dispersion of $N^+C_5Ala2C_{16}$ and $(SO_3^-)C_5Ala2C_{16}$, mixed at the equimolar ratio.

As for the mixed lipid system composed of $N^+C_5Ala2C_{16}$ and $(SO_3^-)C_5Ala2C_{16}$, its turbidity at 30 °C (above T_m) is much sensitive to the lipid composition; the normal bilayer aggregates were spontaneously formed when the composition loses the fractional balance, retained at the equimolar ratio of both lipids, to any slight extent (Fig. 8). The extent of turbidity of the same mixed lipid system was independent of the lipid composition below T_m and comparable to that observed for the bilayer aggregates. The identical correlation of turbidity with lipid composition was also observed for the $N^+C_5Ala2C_{14}$–$(SO_3^-)C_5Ala2C_{14}$ system at 21 °C (above T_m).

X-Ray Diffraction Measurements. The low-angle X-ray diffraction technique was applied to the mixed lipid system composed of $N^+C_5Ala2C_{14}$ and $(SO_3^-)C_5Ala2C_{14}$ at room temperature (15±5 °C). An equimolar mixture of the lipids in water (the weight fraction of the total lipid quantity, 0.40) showed four diffractions consistent with spacings of 88, 75, 53, and 43 Å (Fig. 9A). This spacing ratio ($1:\sqrt{3}/2:\sqrt{3}/\sqrt{8}:1/2$) rules out the occurrence of lamellar and hexagonal phases since these requires the ratios of 1:1/2:1/3:1/4 and $1:1/\sqrt{3}:1/\sqrt{4}:1/\sqrt{7}$, respectively.[9] The present spacing ratio is in conformity with diffractions from (111), (200), (220), and (222) planes of the face-centered cubic (fcc) lattice having a lattice constant (a), 152 Å. The (111) plane of the fcc lattice is the closest packed one, and the distance between the nearest neighbors in the plane ($a/\sqrt{2}$, 108 Å) is referred to the repeating distance of elements (internal aqueous compartments; see Fig. 10) and in good agreement with the values evaluated by electron microscopy.[7] When the weight fraction of the total lipid quantity in water was reduced to 0.20, the $a/\sqrt{2}$ value was slightly increased to give 111 Å. Meanwhile, a mixture of $N^+C_5Ala2C_{14}$ and $(SO_3^-)C_5Ala2C_{14}$ at a molar ratio of 45:55 in water (the weight fraction of the total lipid quantity, 0.17) afforded a single diffraction with spacing of 52 Å (Fig. 9B), which corresponds to the bilayer thickness evaluated from the CPK molecular models.

Discussion

In the course of our studies on model membranes composed of synthetic peptide lipids,[5,6] we have emphasized that the hydrogen-belt domain[10] constructed with amino acid residues in the intramembrane phase contributes much to the morphological stability of such aggregates. The tight intramembrane hydrogen-bonding interaction, which leads to the formation of the hydrogen-belt domain, was confirmed by various spectroscopic measurements.[6b,11] The cationic peptide lipids such as $N^+C_5Ala2C_n$ (n=12—18)

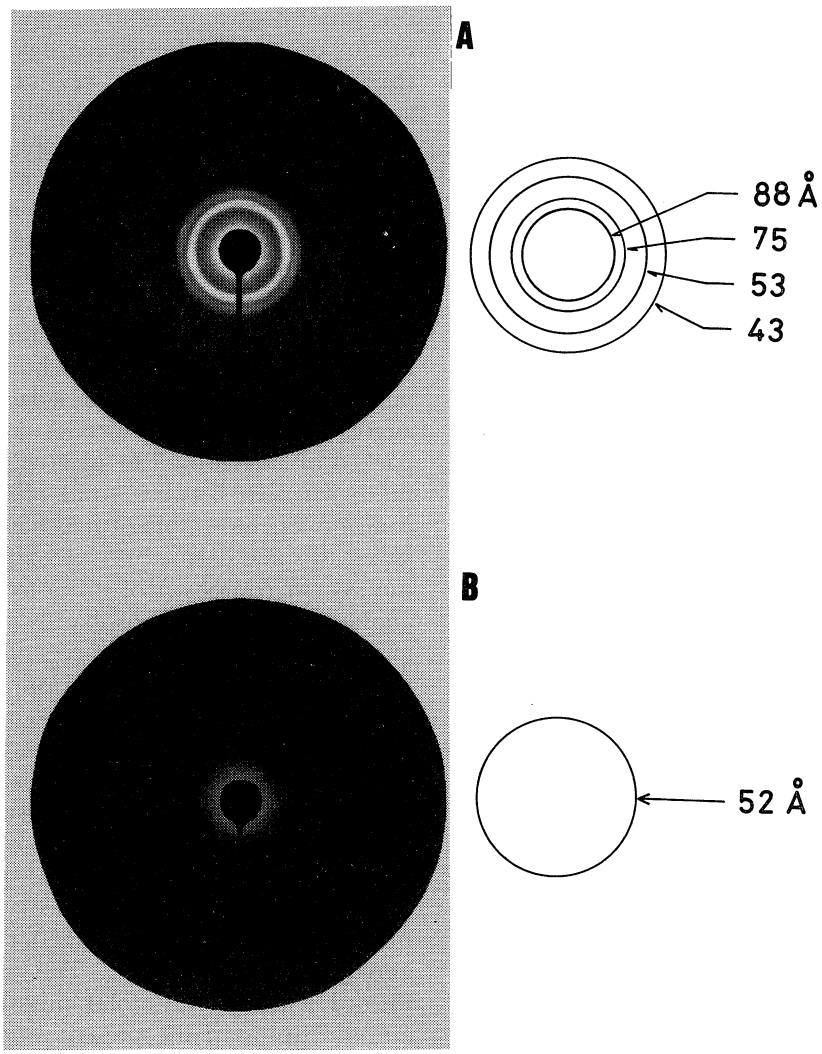

Fig. 9. X-Ray diffraction patterns for the following samples dispersed in water: A, an equimolar mixture of $N^+C_5Ala2C_{14}$ and $(SO_3^-)C_5Ala2C_{14}$ (weight fraction of the total lipid species, 0.40); B, a mixture of $N^+C_5Ala2C_{14}$ and $(SO_3^-)C_5Ala2C_{14}$ at the 45:55 molar ratio (weight fraction of the total lipid species, 0.17).

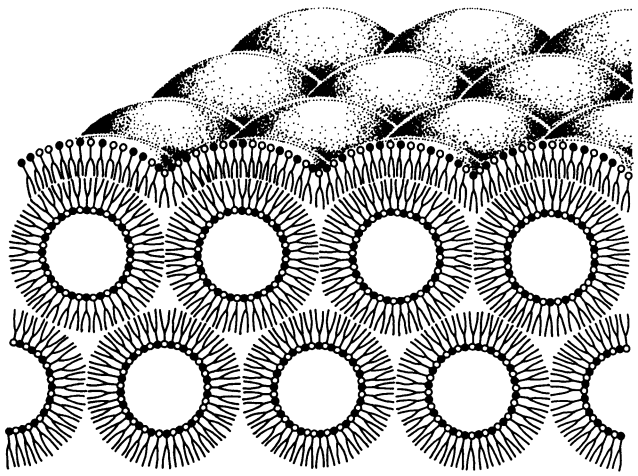

Fig. 10 Schematic representation of the nonlamellar aggregates formed with cationic (O–<) and anionic (●–<) lipids mixed at the equimolar ratio in water. The cross section corresponds to the (111) plane of the fcc lattice.

form multiwalled bilayer aggregates in the aqueous dispersion state, which are then transformed into single-walled vesicles upon sonication.[5c] Such single-walled vesicles are morphologically stable enough to inhibit fusion or aggregation under ordinary conditions.[5c] Regardless of the nature of amino acid residues and ionic head moieties placed in synthetic peptide lipids, the phase transition parameters for these aggregates in the aqueous dispersion state are primarily dependent on the length of the hydrophobic double-chain segment.[6b] On the other hand, nonionic peptide lipids having the quinoyl residue as a polar head moiety, QC_5Ala2C_n, form nonlamellar assemblies with the highly ordered and three-dimensional network arrangement of small aqueous compartments.[6a] Since the phase transition enthalpy (ΔH) and the fluorescence polarization parameter (r_s) obtained with DPH in the gel state for these aggregates are smaller than those for bilayer aggregates having the same double-

chain segments,[6b] the nonlamellar phase seems to be stable regardless of the phase transition.

As for the mixed peptide lipid systems, the bilayer phase is predominantly present under conditions that the total surface charge of the aggregate is not completely neutralized. On the other hand, the nonlamellar phase, schematically shown in Fig. 10, appears in the aqueous dispersions of cationic and anionic lipids mixed at the 1:1 molar ratio above T_m (Figs. 2 and 3). Under the latter conditions, the aggregates retain the high microscopic homogeneity of cationic and anionic lipid molecules (Fig. 5). The achievement of such microscopic homogeneity must be originated from the intramembrane electrostatic interaction between cationic and anionic head moieties to form highly developed ion-pair clusters on the membrane surface. Furthermore, the nonlamellar phase appeared above T_m in the mixed system of cationic and anionic lipids was spontaneously transformed into the normal bilayer phase below T_m as confirmed by the negative staining electron microscopy (Fig. 4). Since the nonlamellar domain is much more extensively developed than the bilayer one, the morphological transition between them was also reflected on turbidity change, accompanied with a hysteresis loop as shown in Fig. 7. In the light of the above observations, the gel to liquid-crystalline transition, which takes place in the hydrophobic domain, is thermodynamically required for transformation of the bilayer phase into the nonbilayer one. The liquid-crystalline bilayer phase, which would appear between the bilayer gel phase and the nonbilayer phase,[1a] was not detected by DSC, fluorescence polarization, and turbidity measurements under ordinary conditions.

It has been proposed that the aggregate morphology, which is favored thermodynamically in aqueous media, is theoretically rationalized in view of the dynamic packing mode of lipid molecules by introducing the critical packing parameter, $v/(a_0 l_c)$; where v, a_0, and l_c are the hydrocarbon volume, optimal surface area, and critical chain length of a lipid molecule, respectively.[12] According to this concept, the nonlamellar structure requires $v/(a_0 l_c)>1$, whereas the bilayer structure is favored under the conditions $1/2<v/(a_0 l_c)<1$. As we have previously discussed, the a_0 value is the primary factor which acts to develop the aggregate morphology observed for QC_5Ala2C_n.[6b] On the other hand, the 1:1 cationic–anionic lipid system develops the bilayer phase in the gel state. Therefore, the average a_0 value seems to be larger than that for QC_5Ala2C_n. However, the critical packing parameter must become larger than 1 in the temperature range above T_m by increasing the v value. This effect is plausibly brought about by defrosting the rotational motion of the hydrophobic double-chain segment.

The formation of *lipidic particles* or *lipidic intramembranous particles* has been detected in various aqueous lipid mixtures and in total lipid extracts under physiological conditions by means of electron microscopy.[2] Globular aggregates are arranged in three-dimensional quasi-crystalline manners and associated to afford various lipidic particles, showing large variation in shape, size, and packing behavior, as observed for the following mixed lipid systems: cardiolipin and egg phosphatidylcholine in the presence of calcium ions,[3a] monogalactosyldiacylglycerol and digalactosyldiacylglycerol,[3f] cardiolipin and chlorpromazine,[13] dioleoylphosphatidic acid and chlorpromazine,[13] and dilinoleoylphosphatidylethanolamine and egg phosphatidylcholine.[14] The lipidic particle phase has been suggested to consist of spherical aggregates of inverted micelles arranged in a closely packed organization[13] or to involve inverted micelles sandwiched in between lipid bilayers.[3f] These two concepts on morphological behavior have been subjected to some debate.[14,15] An aggregation mode for the system composed of dilinoleoylphosphatidylethanolamine and egg phosphatidylcholine at the 85:15 molar ratio in the quasi-crystalline state, in fact, was consistent with an isotropic cubic phase[14] in a manner as observed for systems composed of ordinary detergents such as potassium carboxylates and quaternary ammonium halides bearing a long alkyl chain[16] and of monoglycerides such as 1-monoolein and 1-monostearin,[17] all being based on the X-ray diffraction method. Such lipidic particles have been often observed in an intermediate step during the phase transition between lamellar and inverted hexagonal (H_{II}) phases.[14,18] The globular aggregates formed with an equimolar mixture of cationic and anionic lipids in the present study apparently constitute a highly developed quasi-crystalline phase with the face-centered cubic lattice. However, this phase remains stable in the aqueous dispersion state without being transformed into the H_{II} phase under the present conditions. The previous studies with mixed lipid systems, which allow the formation of lipidic particles, claimed that one of the mixed lipid species at least needs to prefer to constitute the H_{II} phase for each mixed system when it is dispersed in water alone.[2] However, this concept must be revised since lipidic particles are also formed with two kinds of lipids which constitute individually normal bilayer aggregates in the aqueous dispersion state. Thus, the formation of globular aggregates is primarily controlled by the critical packing parameter, which is subjected to change by the intramembrane interaction mode among the polar head moieties and/or the rotational freedom of the hydrophobic double-chain segment of lipid species. However, the molecular basis for the formation of various three-dimensional quasi-crystalline phases, such as inverted hexagonal and inverted cubic, needs to be clarified by employing appropriate synthetic lipids. Since it has been suggested that lipidic particles assume important roles in membrane fusion and trans-membrane transport,[2]

the present nonbilayer systems may provide useful means for clarifying those mechanisms.

We are grateful to professor Tisato Kajiyama of Kyushu University for the X-ray diffraction measurements. The present work was supported in part by a Grant-in-Aid for Scientific Research from the Ministry of Education, Science, and Culture (No. 58430016).

References

1) a) P. R. Cullis and B. De Kruijff, *Biochim. Biophys. Acta*, **559**, 399 (1979); b) S. W. Hui, T. P. Stewart, and L. T. Boni, *Chem. Phys. Lipids*, **33**, 113 (1983).

2) A. J. Verkleij, *Biochim. Biophys. Acta*, **779**, 43 (1984).

3) a) A. J. Verkleij, C. Mombers, W. J. Gerritsen, L. Leunissen-Bijvelt, and P. R. Cullis, *Biochim. Biophys. Acta*, **555**, 358 (1979); b) R. G. Miller, *Nature (London)*, **287**, 166 (1980); c) S. W. Hui, T. P. Stewart, and L. T. Boni, *Science*, **212**, 921 (1981); d) E. L. Bearer, N. Düzgünes, D. S. Friend, and D. Papahadjopoulos, *Biochim. Biophys. Acta*, **693**, 93 (1982); e) B. Kachar and T. S. Reese, *Nature (London)*, **296**, 464 (1982); f) P. J. Quinn and W. P. Williams, *Biochim. Biophys. Acta*, **737**, 223 (1983).

4) J. H. Fendler, "Membrane Mimetic Chemistry," John Wiley, New York (1982), Chap. 6 and 12.

5) a) Y. Murakami, A. Nakano, and K. Fukuya, *J. Am. Chem. Soc.*, **102**, 4253 (1980); b) Y. Murakami, A. Nakano, and H. Ikeda, *J. Org. Chem.*, **47**, 2137 (1982); c) Y. Murakami, A. Nakano, A. Yoshimatsu, K. Uchitomi, and Y. Matsuda, *J. Am. Chem. Soc.*, **106**, 3613 (1984).

6) a) Y. Murakami, A. Nakano, J. Kikuchi, T. Takaki, and K. Uchimura, *Chem. Lett.*, **1983**, 1891; b) Y. Murakami, J. Kikuchi, T. Takaki, K. Uchimura, and A. Nakano, *J. Am. Chem. Soc.*, **107**, 2161 (1985).

7) Y. Murakami, J. Kikuchi, T. Takaki, and K. Uchimura, *J. Am. Chem. Soc.*, **107**, 3373 (1985).

8) The pH effect on the aggregate morphology of NC_5Ala2C_n will be reported elsewhere. In the present work, this lipid was used under acidic conditions below pH 6 so as to behave as a cationic one [$N^+(H)C_5Ala2C_n$].

9) V. Luzzati, H. Mustacchi, A. Skoulios, and F. Husson, *Acta Cryst.*, **13**, 660 (1960).

10) H. Brockerhoff, "Bioorganic Chemistry," ed by E. E. van Tamelen, Academic Press, New York (1977), Vol. 3, Chap. 1.

11) a) Y. Murakami, Y. Aoyama, A. Nakano, T. Tada, and K. Fukuya, *J. Am. Chem. Soc.*, **103**, 3951 (1981); b) Y. Murakami, A. Nakano, and A. Yoshimatsu, *Chem. Lett.*, **1984**, 13.

12) a) J. N. Israelachvili, D. J. Mitchell, and B. W. Ninham, *J. Chem. Soc., Faraday Trans. 2*, **72**, 1525 (1976); b) J. N. Israelachvili, S. Marčelja, and R. G. Horn, *Quart. Rev. Biophys.*, **13**, 121 (1980).

13) A. J. Verkleij, R. De Maagd, J. Leunissen-Bijvelt, and B. De Kruijff, *Biochim. Biophys. Acta*, **684**, 255 (1982).

14) S. W. Hui and L. T. Boni, *Nature (London)*, **296**, 175 (1982).

15) W. P. Williams, A. Sen, A. P. R. Brain, P. J. Quinn, and M. J. Dickens, *Nature (London)*, **296**, 175 (1982).

16) V. Luzzati and F. Reiss-Husson, *Nature (London)*, **210**, 1351 (1966).

17) G. Lindblom, K. Larsson, L. Johansson, K. Fontell, and S. Forsén, *J. Am. Chem. Soc.*, **101**, 5465 (1979).

18) R. van Venetië and A. J. Verkleij, *Biochim. Biophys. Acta*, **645**, 262 (1981).